



	<b>Experiment title:</b> Following the LPMO Active Site Throughout Productive-Pathway Turnover: Characterization of Chitin-Bound Intermediates	<b>Experiment number:</b> CH 6601
<b>Beamline:</b> BM23	<b>Date of experiment:</b> from: 07 Jun 2023 to: 12 Jun 2023	<b>Date of report:</b> 22 Dec 2023
<b>Shifts:</b> 12	<b>Local contact(s):</b> Cesare Atzori	<i>Received at ESRF:</i>
<b>Names and affiliations of applicants</b> (* indicates experimentalists): Chris Joseph* — Max Planck Institute for Chemical Energy Conversion Liqun Kang* — Max Planck Institute for Chemical Energy Conversion Kushal Sengupta* — Max Planck Institute for Chemical Energy Conversion Serena DeBeer — Max Planck Institute for Chemical Energy Conversion		

## Report:

Lytic polysaccharide monooxygenases (LPMOs) are a class of C–H activating Cu metalloenzymes which play an important role in biomass decomposition processes needed to maintain a net-neutral carbon cycle. Utilizing room temperature X-band EPR (Electron Paramagnetic Resonance) Spectroscopy, we recently developed a method by which relevant timepoints for the freeze-quenched isolation of LPMO under turnover conditions (with O<sub>2</sub>) can be determined for obtaining samples catalytically-relevant copper-oxo intermediates. However, while the EPR strategy is a useful method for following Cbp21 as it progresses through turnover, the presence of EPR-silent reaction sites renders characterization of these intermediates impossible by this technique. Furthermore, the heterogeneous, chitinous sample environment is not amenable to a number of the typical inorganic spectroscopy techniques (*e.g.* UV-vis, MCD). In contrast, Cu K-edge XAS is uniquely suited to characterize such intermediates. Thus, we wished to pursue Cu K-edge XAS as a consistent method amenable to the characterization of chitin-bound LPMO (Cu<sup>II</sup> and Cu<sup>I</sup>).

Overall, the beamline available at BM23 did provide a stable beam and consistently reproducible scans. The beamline was configured with the Si(111) double crystal monochromator for upstream energy selection. A typical issue with dilute protein samples is diffraction caused by ice crystals, necessitating an energy-resolving multielement fluorescence detector with individually-resolved channels. However, the 13-element Ge detector was unavailable for the experiment. In lieu of the multielement Ge detector stood the 4-element Hitachi Vortex-EX SDD detector (coupled with Falcon readout electronics). However, we found that the large beam footprint of 0.5 mm × 2 mm (v × h, slitted) significantly assuaged any apparent (or at least severe) ice diffraction issues.

In this experiment, the Cu(II) protein samples were particularly prone to X-ray induced photodamage, as has been found in previous synchrotron X-ray experiments. To mitigate this, a cryostat was installed into the beamline configuration to maintain sample temperatures of ~15 K. However, we found that some issues related to the use of the cryostat which hindered the experiment. First, loading samples which are frozen prior to sample mounting into the cryostat proves difficult if maintaining a cold sample throughout the mounting process is desired. The mounting process requires that samples spend on the order of 1–2 minutes at room temperatures while vacuum/He cycling the atmosphere during the transfer process. During this time, it is quite likely that the

sample temperature becomes quite high. Thus, when mounting samples of freeze-quenched turnover intermediates, it cannot be ascertained that the sample composition has not changed during the loading procedure. Secondly, the rod of the cryostat was made from PEEK material. This has the advantage of providing a more metal-free cryostat environment. However, we also discovered a disadvantage in using this system. Upon being transferred from room temperature into the 15 K cryostat environment, all materials naturally undergo a thermal compression until an equilibrium is reached specific to that material. In our past experiment with aluminum rods, we found that the rod would reach this equilibrium fairly quickly, and the first few alignment scans could reliably represent sample positions throughout the experiment. With the PEEK rod, we found that it took hours for the rod to reach thermal equilibrium and that sample positions could not be reliably reproduced during that time (Figure 1), with the most severe changes happening in the first hours after mounting. In order to address long lag-time until the rod reached equilibrium and guarantee a fresh sample spot with each scan, a script was written such that an alignment scan was performed before each XAFS scan, and the expected sample position could be compared and adjusted against the actual position.

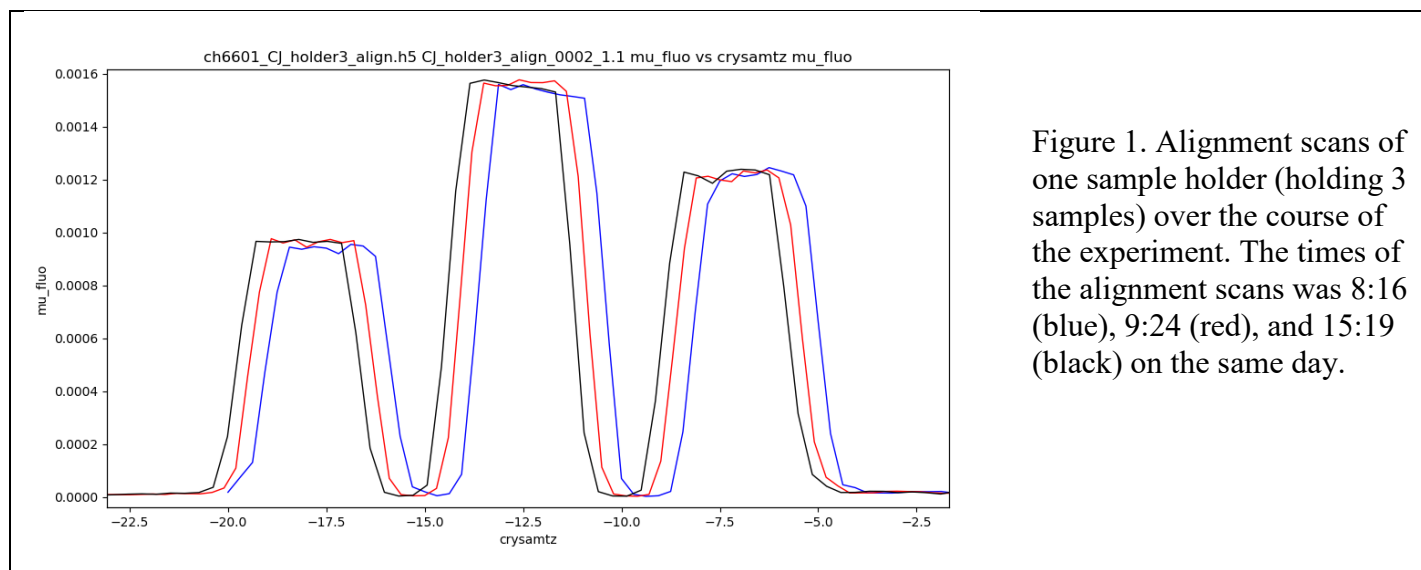


Figure 1. Alignment scans of one sample holder (holding 3 samples) over the course of the experiment. The times of the alignment scans was 8:16 (blue), 9:24 (red), and 15:19 (black) on the same day.

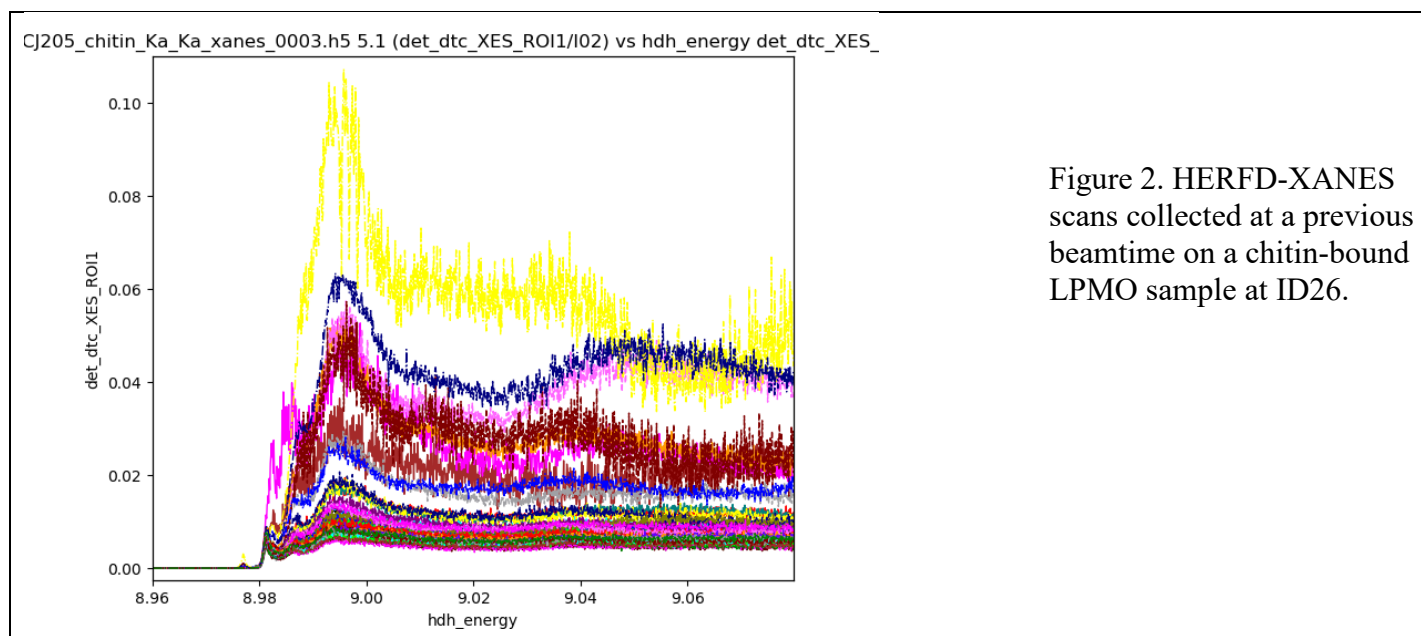


Figure 2. HERFD-XANES scans collected at a previous beamtime on a chitin-bound LPMO sample at ID26.

The intended samples for this beamtime were chitin-bound LPMO samples. These samples are notoriously inhomogenous, which has been demonstrated previously by the spot-dependent variability between scans at ID26 (Figure 2). Thus, we believed that collecting reliable data on such inhomogenous samples, considering that the sample moves slightly during the scan (due to thermal compression of the PEEK rod), would be difficult, and the reliability of the data would be difficult to ascertain. However, in order to take advantage of the capabilities of BM23 and apply it to LPMO-related work, we pursued the collection of data of the enzyme in its resting and reduced states under various pH conditions. We have recently found (by EPR) that the LPMO

undergoes a pH-dependent transition event with an equilibrium point near pH 8. This has consequences for understanding the optimal reaction conditions for the catalytic operation of the enzyme. Thus, Cu(2+) and Cu(1+) LPMOs were prepared in pH 6.5 and pH 11.5 conditions. We found that BM23 is perfectly capable of collecting excellent XANES data on these homogenous, frozen protein samples. We were particularly pleased at the competence of BM23 to collect on Cu(2+) protein samples without any observable X-ray induced photodamage (Figure 3). In addition, Cu(1+) data was collected, for which the pH-dependent transition event is not expected (Figure 4).

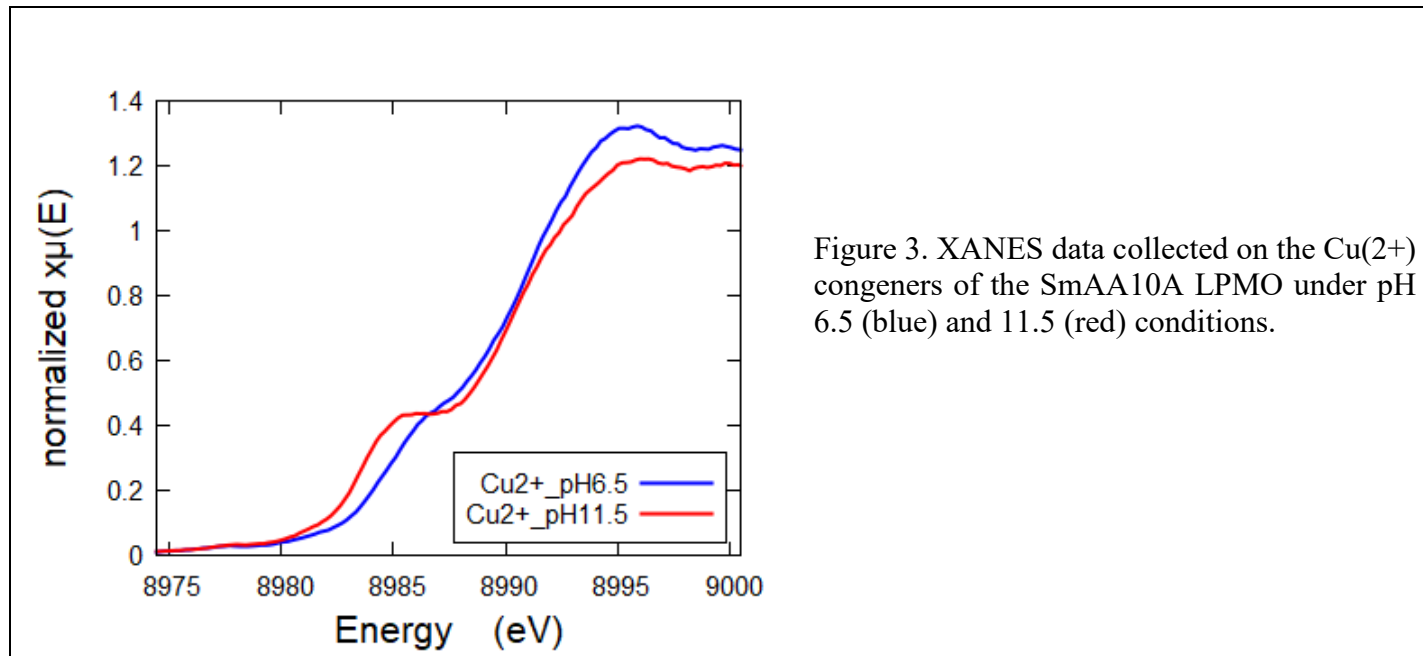


Figure 3. XANES data collected on the Cu(2+) congeners of the SmAA10A LPMO under pH 6.5 (blue) and 11.5 (red) conditions.

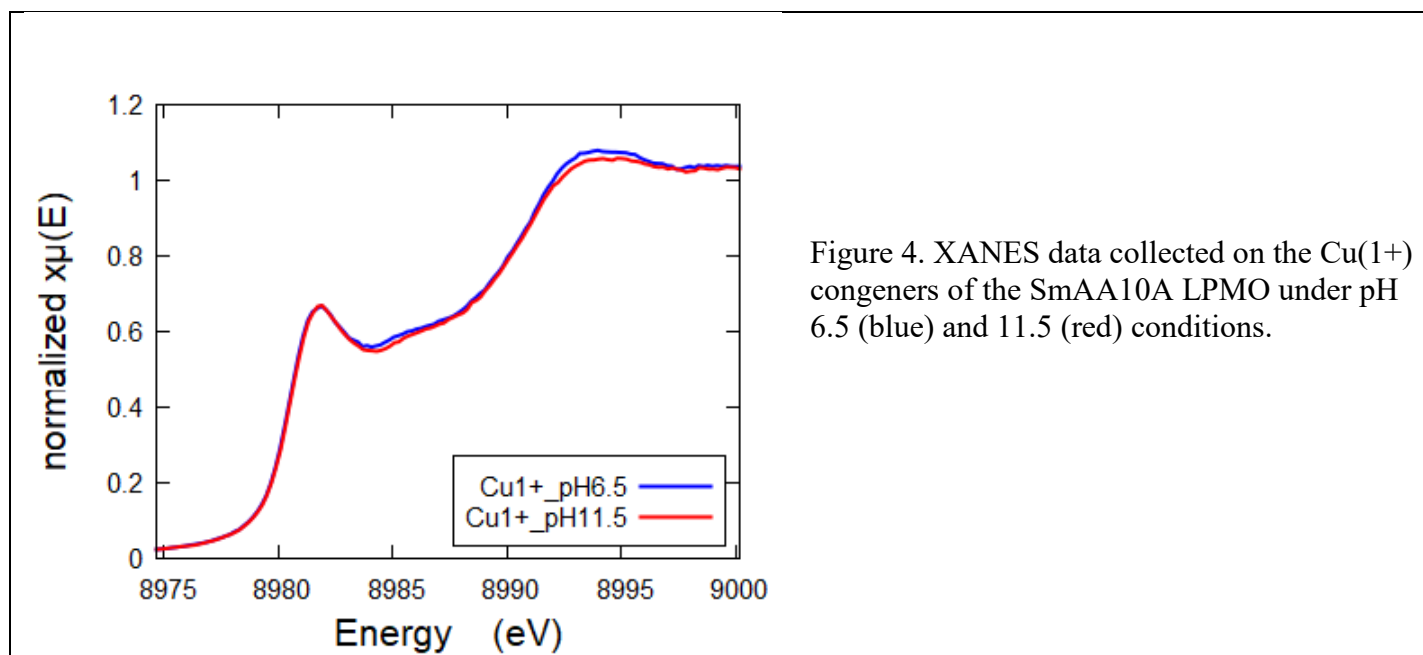


Figure 4. XANES data collected on the Cu(1+) congeners of the SmAA10A LPMO under pH 6.5 (blue) and 11.5 (red) conditions.

In addition to the Cu K-edge samples, we attempted to collect on an Fe metalloprotein. The BM23 beamline was found to be perfectly competent at the fast collection of XANES (Figure 5); however, the collection of high-quality EXAFS data would have been extremely time-consuming.

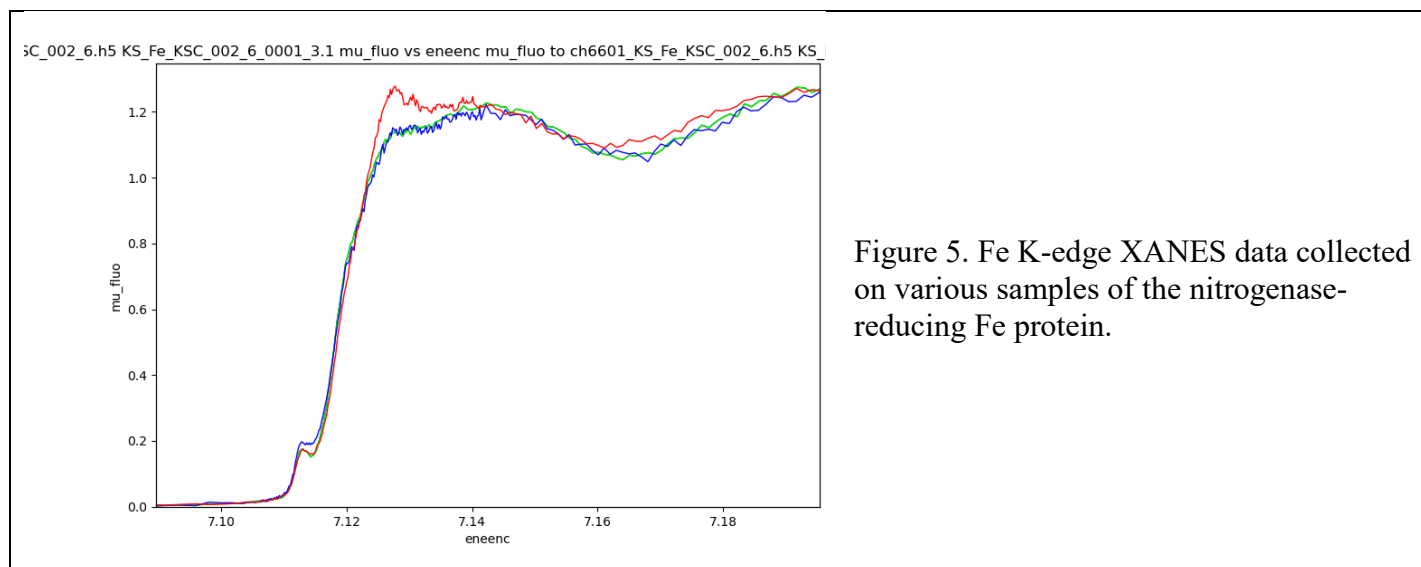


Figure 5. Fe K-edge XANES data collected on various samples of the nitrogenase-reducing Fe protein.

Lastly, we were able to take full advantage of the capabilities of BM23 with the collection of both XANES and EXAFS data on a slew of solid samples for transmission experiments (Fe K-edge). These samples included various small molecule compounds (Figure 6), as well as several materials samples (not shown).

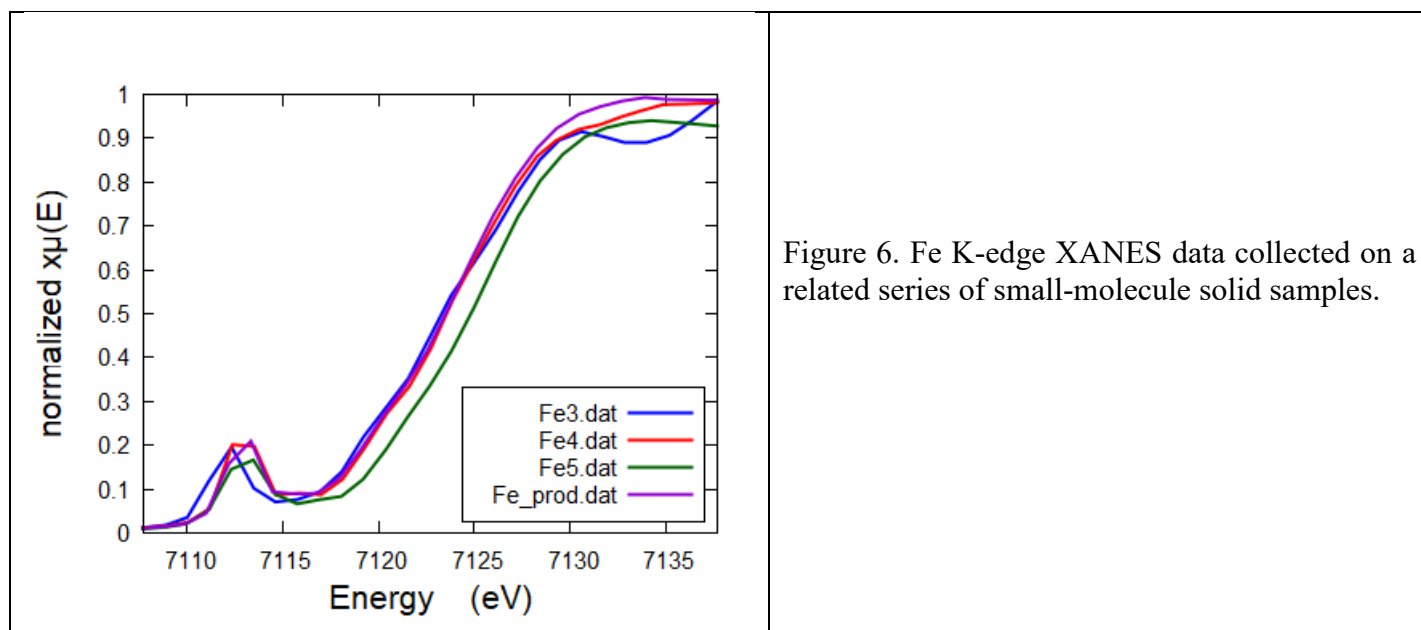


Figure 6. Fe K-edge XANES data collected on a related series of small-molecule solid samples.